A Computational Study on the Stacking Interaction in Quinhydrone

María J. González Moa, Marcos Mandado, and Ricardo A. Mosquera*

Dpto. Química Física, Facultade de Química, Universidade de Vigo, Lagoas-Marcosende s/n, 36310-Vigo, Galicia, Spain

Received: September 20, 2006; In Final Form: December 15, 2006

The stability and electron density topology of quinhydrone complex was studied using multiple computational levels, including MPW1B95 Truhlar's density functional. The QTAIM analysis demonstrates that an electron population transfer from hydroquinone to quinone monomer accompanies the complex formation. The variations undergone by atomic populations indicate that the electron transfer through HOMO LUMO overlap is combined with a reorganization of the electron density within each monomer. Variations of two- and six-center delocalization indices show a small reduction of electron delocalization in the hydroquinone ring upon complex formation.

Introduction

Aromatic π-stacking interactions play an important role in chemistry and biology.[1,2] They are fundamental for the geometry characteristics and stabilization energy of DNA molecules, the crystal packing of aromatic molecules, the formation of the tertiary structure of proteins, the control in the enzyme−nucleic acids recognition regulating gene expression, intercalation of drugs into DNA, and so on. For that reason, the stacking interactions were, and still are, the subject of numerous works.[3−8] π-stacking in the benzene dimer has been widely studied[9−13] as a prototype of these interactions.

Charge transfer (CT) between monomers has been frequently used to explain the stability of π-stacking complexes. Thus, the study of CT in π-stacks has attracted considerable attention.[14] An important example of such processes is charge migration in DNA, which has been studied both theoretically and experimentally.[15] Nevertheless, to the best of our knowledge, no quantitative measurement of the CT in stacking complexes has been made. A simpler example of molecular CT system is the well-known benzoquinone−hydroquinone complex (quinhydrone). In this complex, the CT between the electron donor (hydroquinone) and the electron acceptor (quinone) is generally considered as the primary source for complex stabilization, while the hydrogen bonds provide additional stability both in the solid state and in solution.[16] Nevertheless, a previous computational study on quinhydrone using the MP2/6-31G(d) level and NBO analysis for estimating the CT interaction energy was unable to conclude the leading role of this factor in the complex stabilization.[17] According to Mulliken's overlap and orientation principle, the geometry of CT complexes is conditioned by obtaining the maximum overlap of the filled donor molecular orbital (HOMO) and the vacant acceptor orbital (LUMO).[18]

CCSD(T) calculations have proved to describe stacking complexes accurately.[19] Nevertheless, the size of stacking complexes is usually large, and it is not practical to employ high level ab initio calculations to study them. Even, MP2 calculations are not adequate to describe this kind of systems, as they usually overestimate complex stability.[19] Density functional theory methods provide generally a reasonable balance of accuracy and computational cost, so they are an important tool for studying biological systems. Nevertheless, the most popular DFT method, B3LYP, cannot describe stacking interactions because it fails for dispersion interactions. However, a new generation of density functional methods developed by Truhlar and co-workers[20−23] has shown to describe $\pi-\pi$ interactions in stacked DNA base pairs and amino acid pairs. The two key innovations of the new functionals are that they include kinetic energy density and have a more physical dependence on the reduced density gradient in the region important for weak interactions.

In this work we compare the stacking energy afforded by Truhlar's functionals, with that ones obtained from other methods that are used to describe $\pi-\pi$ stacked complexes and the experimental value,[24] for the simple quinone-hydroquinone complex. Also, from the density described by Truhlar's functionals, we have measured the charge-transfer that takes place within the complex. To accomplish this, we have analyzed the interactions and the charge movements between the two molecules in the framework of Bader's quantum theory of atoms in molecules (QTAIM).[25,26] Comparison of QTAIM atomic populations in the complex and monomers allows testing the reliability of Mulliken's overlap and orientation principle. Finally, we have calculated the change in the electron delocalization within each molecule in the dimer employing QTAIM two-center delocalization indices[27] and the recently introduced *n*-center delocalization indices.[28]

Computational Details. Single-point calculations at HF, MP2, B3LYP, and Truhlar's density functionals MPW1B95 and MPWB1K[23] levels were carried out using 6-311++G(2d,2p) 6d as a basis set with Gaussian 03 program[29] for the quinone−hydroquinone dimer, considering the geometry described for the quinhydrone crystal.[30] Even though the pairs in the crystal do not necessary correspond to the lowest-energy arrangements in the gas-phase dimer, as it happens to benzene dimer,[31] it will work as a good estimation for the purpose of this work. Counterpoise correction for basis set superposition error was only performed at the HF, MP2, and B3LYP levels, as MPW1B95 and MPWB1K functionals were developed in such a way that they give reasonable results for noncovalent interactions both with and without counterpoise corrections, and the developers pointed out that they should be useable without the need of counterpoise corrections, especially when the basis

10.1021/jp0661701 CCC: $37.00
Published on Web 02/20/2007

TABLE 1: Molecular Energies of Quinone, Hydroquinone and Dimer in au and Stacking Energies in kcal·mol^{-1} Using Different Levels of Calculation and the Basis Sets Indicated.

	quinone (Q)	hidroquinone (H)	dimer	stacking energy
HF[a]	−379.34136	−380.52184	−759.85562[c]	4.76[c]
B3LYP[a]	−381.57671	−382.81064	−764.38402[c]	2.09[c]
MPWB1K[a]	−381.43286	−382.67659	−764.10979	−0.22
MPW1B95[a]	−381.41178	−382.64062	−764.05685	−2.80
MPW1B95[b]	−381.42811	−382.65832	−764.09001	−2.25
BH&H[a]	−378.93159	−380.14158	−759.08290[c]	−6.11
MP2[a]	−380.61026	−381.83473	−762.45596[c]	−6.89[c]
SCS-MP2[a]	−380.57363	−381.79310	−762.37885	−7.61

[a] 6-311++G (2d,2p) 6d. [b] AUG-cc-pVTZ. [c] This calculation includes the correction to the BSSE.

is triple-ζ quality or better (as it is here). In order to compare results, single-point calculations on the crystal geometry were also carried out at the same levels and using the same basis set for the quinone and hydroquinone monomers. In each molecule, the QTAIM charge density analysis was performed with the AIMPAC[32] package of programs and AIM2000.[33]

This work is focused on atomic populations, $N(\Omega)$, and the properties at the bond critical points (BCP) of the electron density.[25,26] $N(\Omega)$ values were calculated for MP2, B3LYP and MPW1B95 electron densities. The accuracy obtained in their determination was checked using standard criteria. Thus, summations of $N(\Omega)$ and atomic energy, $E(\Omega)$, values for each molecule reproduce total electron populations and electronic molecular energies below $5\cdot10^{-3}$ au and 3.2 kJ mol^{-1}, respectively. No atom was integrated with absolute values of the $L(\Omega)$ function[25,26] larger than $2\cdot10^{-3}$ au.

Stacking Energies. Molecular energies computed at the levels here studied for quinone and hydroquinone isolated molecules and quinhydrone complex were used to calculate the stacking energy of quinhydrone (Table 1). The first two methods, HF and B3LYP, as could be expected from previous studies on other systems,[7,34−36] give rise to an unstable dimer. On the opposite side, as it also happens to DNA base pairs,[20] MP2 level furnishes a high stacking energy, although it is well-known that MP2 calculations greatly overestimate the stabilization energy.[19] The hybrid BH&H level[37] produces a stacking energy close to that of MP2, and when we use the correction proposed by Grimme[38] for MP2 the stacking complex results even more stabilized than with standard MP2. Finally, both Truhlar's density functionals give rise to stable quinhydrone with not so high stacking energy. In fact, the MPW1B95/6-311++G(2d,2p) 6d value for the stacking energy agrees with the experimental data (2.8 ± 0.1 kcal.mol^{-1})[24] and that obtained with the same functional and the AUG-cc-pVTZ basis set differs from the experimental value by less than 0.6 kcal.mol^{-1} (Table 1).

QTAIM Analysis. The QTAIM analysis of the electron density obtained for the dimer at any of the computational levels here considered reveals the presence of 4 intermolecular BCP's. Two of them correspond to C···C weak interactions and two to C···O ones, the former showing higher density at the BCP's. All of them exhibit $\rho(\mathbf{r}_c)$ (between $4\cdot10^{-3}$ and $7\cdot10^{-3}$ au) and total electronic energy density, $H(\mathbf{r}_c)$, (around $1\cdot10^{-3}$ au) values similar to those found in previous QTAIM works on stacking interactions in DNA bases.[5] Nevertheless, in this case we observe negative $\nabla^2\rho(\mathbf{r}_c)$ values and quite large differences between bond path lengths and internuclear distances (Table 2). If we exclude the B3LYP electron density (where the intermolecular bond path at the oxygen of hydroquinone is connected to the ipso carbon of quinone), all the electron distributions provide the same chemical graph (Figure 1).

TABLE 2: Main Properties of the Intermolecular Critical Points (in au, See Figure 1 for Nomenclature), Internuclear Distance (R), and Difference between Bondpath Length and *R*, Δ*R*, (in Å) Associated to Every Intermolecular BCP

	$10^3\,\rho(\mathbf{r}_c)$	$10^3\,\nabla^2\rho(\mathbf{r}_c)$	$10^3\,H(\mathbf{r}_c)$	R	Δ*R*	$10^3\,\delta$[a]
B1	7.0	−5.2	1.2	3.375	0.331	1.3
B2	7.4	−5.3	1.2	3.242	0.565	2.8
B3	6.4	−5.7	1.1	3.269	0.231	2.2
B4	4.4	−3.7	0.7	3.423	0.115	1.7
R1	5.3	−4.8	0.9			
R2	5.1	−4.5	0.8			
R3	6.9	−5.7	1.3			
R4	4.2	−3.7	0.7			
R5	4.1	−3.7	0.7			
C1	3.7	−3.9	0.8			
C2	4.4	−4.3	0.9			

[a] Two-center delocalization index (in au).

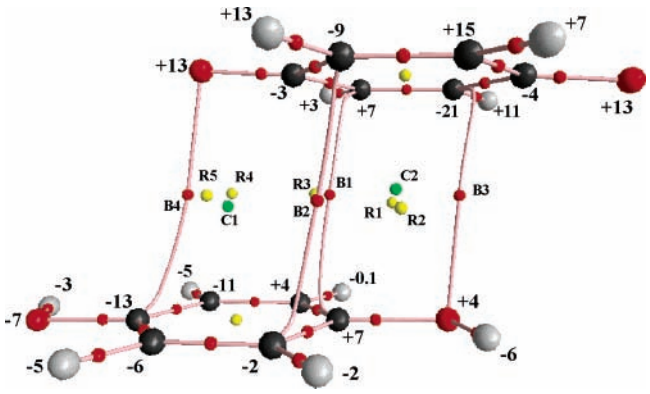

Figure 1. Quinhydrone molecular graph (obtained with AIM-2000[33]) indicating the variations of the atomic electron population computed with MPW1B95 functional density. All values multiplied by 10^3 and in au.

The set of weak bonds established are accompanied by some noticeable modifications of the atomic properties of the monomers in quinhydrone adduct. Thus, when we compare the population of the isolated molecules to that of the dimer (computed only at the MPW1B95), there is an electron population transfer of 0.046 au from hydroquinone to quinone. Confirming the character of CT complex traditionally assigned to this adduct.[9] The analysis of the atomic population variations, $\Delta N(\Omega)$, (Figure 1) shows that the carbon atoms of one molecule bonded to an oxygen atom of the other molecule are the atoms that experience the highest loss. Also, all the hydrogens belonging to the donor molecule lose electron density, while all the hydrogens in the acceptor molecule gain electron density.

Figure 2 shows the HOMO and LUMO calculated for hydroquinone and quinone monomers, respectively. As it can be observed, in the case of hydroquinone the carbon atoms in trans to hydroxyl do not participate in HOMO, while all the carbons participate in the LUMO of quinone. This would explain why the bonding does not occur always between atoms that are in the same vertical. Although some of the atoms having the largest variations of $N(\Omega)$ also present a significant HOMO−LUMO overlap and participate in the intermolecular bondpaths, it has to be noticed that there are other atoms showing significant $\Delta N(\Omega)$ (Figure 1). Therefore, Mulliken's overlap and orientation principle should be combined with a reorganization of electron density within each monomer to get the final atomic populations in the complex.

The two-center delocalization indices, δ, between nonbonded atoms of the same monomer are scarcely reduced in the complex (0.001 au by average and never more than 0.006 au). In general,

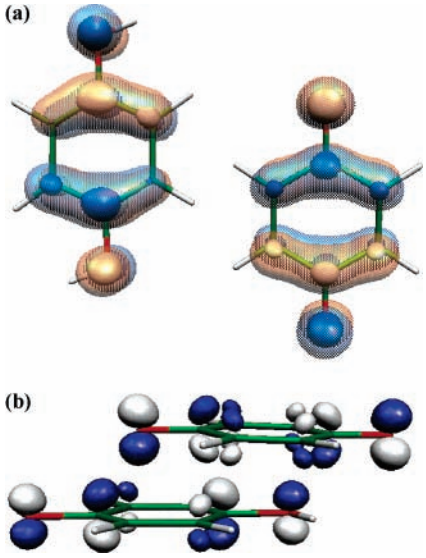

Figure 2. ±0.1 (solid) and ± 0.05 (transparent) isosurfaces of the Kohn−Sham HOMO obtained for hydroquinone molecule and LUMO for quinone at the MPW1B95/6-311++G(2d,2p) 6d level (a). Side view of both MOs (±0.1 contours) in the crystal geometry (b). All images were plotted with MOLEKEL program.[40,41] Blue represents positive values and gray negative ones.

the largest reductions are experienced by pairs that include at least one atom involved in intermolecular stacking bond paths. We also observe the presence of some noticeable delocalizations (δ from 0.010 to 0.028 au) between atoms placed in different monomers. They correspond to the four pairs of atoms connected by the intermolecular bond paths (Table 2) and their neighbors.

The six-center delocalization indices, Δ_6, calculated for each of the C_6 rings in the complex and monomers indicate a noticeable reduction of the local aromaticity of the C_6 ring of hydroquinone upon complex formation. Thus, it goes from 0.0218 au in the monomer to 0.0201 au in the complex. In contrast, the C_6 quinone ring (substantially less aromatic) displays the same Δ_6 value (0.0018 au) in both cases. Overall, the formation of quinhydrone complex is accompanied by a loss of electron density and electron delocalization in the hydroquinone ring. On the other hand, the electron density gained by quinone in the complex is not reflected by the increase of any delocalization index within this unit. Besides, noticeable two-center delocalizations appear between both monomers in the complex.

The slight modifications experienced by $N(\Omega)$ do not alter any important characteristic of each monomer in the adduct. Therefore, quinone shows a strong positive charge on the carbonylic carbon, of around 1 au with any computational level, while the oxygen atoms have even stronger negative charge (Table 3). This extra charge is donated by the hydrogens (0.058 to 0.073 au, depending on the computational level). In all three levels, the results are similar and we have only found some differences at the MP2 level, where the atoms with the highest charge present even higher charge (carbonylic carbons and oxygens), as usual when comparing MP2 and DFT results.[39]

Hydroquinone also displays a similar behavior in the three levels of calculation (the highest differences among methods occur in the carboxylic carbons and oxygen atoms whose charges are again enlarged at the MP2 level). In this case, the carbons bonded to the oxygens display around 0.5 au of positive charge, while the hydroxylic hydrogens have a charge of 0.6 au, so the oxygens have a similar negative charge to the ones in the quinone molecule.

TABLE 3: Atomic Charges in Quinone (Q) and Hydroquinone (H) Monomers (in au)

		$q^{MP2}(\Omega)$	$q^{B3LYP}(\Omega)$	$q^{MPW1B95}(\Omega)$
Q	C[a]	1.122	0.958	0.951
Q	C[b]	−0.003	−0.012	−0.022
Q	H	0.058	0.060	0.073
Q	O	−1.232	−1.050	−1.055
H	C[c]	0.569	0.490	0.440
H	C[d]	0.026	−0.006	−0.026
H	C[e]	0.049	0.012	0.034
H	H[f]	0.624	0.565	0.575
H	H[g]	−0.017	0.000	0.028
H	H[h]	0.019	0.030	0.046
H	O	−1.270	−1.090	−1.097

[a] Carbonyl carbon. [b] Ortho carbon. [c] Ipso carbon. [d] Z-ortho carbon. [e] E-ortho carbon. [f] Hydroxylic hydrogen. [g] Z-ortho hydrogen. [h] E-ortho hydrogen.

Conclusions

The study of quinhydrone complex using the MPW1B95 functional developed by Truhlar et al. allows a good reproduction of its stacking energy at a low computational cost. The QTAIM analysis of the electron density reveals the presence of four interatomic bondpaths and slight, but noticeable, electron population transfer from hydroquinone to quinone in the complex. The variations displayed by atomic populations indicate that the electron transfer through HOMO LUMO overlap is combined with a reorganization of the electron density within each monomer of the complex. The formation of quinhydrone complex takes place with a loss of electron delocalization in the hydroquinone ring not accompanied by the increase of any delocalization index in the quinone ring. Finally, noticeable two-center delocalizations appear between both monomers in the complex.

Acknowledgment. We thank CESGA for access to its computational facilities and financial support from Xunta de Galicia. Helpful suggestions from Dr. J.M. Hermida-Ramón are deeply acknowledged.

References and Notes

(1) Müller-Dethlefs, K.; Hobza, P. *Chem. Rev.* **2000**, *100*, 143.
(2) Hunter, C. A.; Lawson, K. R.; Perkins, J.; Urch, C. J. *J. Chem. Soc., Perkin Trans. 2* **2001**, 651.
(3) Zhikol, O. A.; Shishkin, O. V.; Lyssenko, K. A.; Leszczynski, J. *J. Chem. Phys.* **2005**, *122*, 144104−1.
(4) Tauer, T. P.; Sherrill, C. D. *J. Phys. Chem. A* **2005**, *209*, 10475.
(5) Matta, C. F.; Castillo, N.; Boyd, R. J. *J. Phys. Chem. B* **2006**, *110*, 563.
(6) Cysewski, P.; Czyznikowska-Balcerak, Z *J. Mol. Struct. THEOCHEM* **2005**, *757*, 29.
(7) Tsuzuki, S.; Honda, K.; Azumi, R. *J. Am. Chem. Soc.* **2002**, *124*, 12200.
(8) Manojkumar, T. K.; Choi, H. S.; Hong, B. H.; Tarakeshwar, P.; Kim, K. S. *J. Chem. Phys.* **2004**, *121*, 841.
(9) Hobza, P.; Selzle, H. L.; Schlag, E. W. *J. Am. Chem. Soc.* **1994**, *116*, 3500.
(10) Jaffe, R. L.; Smith, G. D. *J. Chem. Phys.* **1996**, *105*, 2780.
(11) Spirko, V.; Engkvist, O.; Soldan, P.; Selzle, H. L.; Schlag, Hobza, P. *J. Chem. Phys.* **1999**, *111*, 572.
(12) Zhikol, O. A.; Shishkin, O. V.; Lyssenko, K. A.; Leszczynski, J. *J. Chem. Phys.* **2005**, *122*, 144104−1.
(13) Sinnokrot, M. O.; Sherril, C. D. *J. Phys. Chem. A* **2006**, *110*, 10656.
(14) Voityuk, A. A. *Chem. Phys. Lett.* **2006**, *422*, 15.
(15) Long-range charge transfer in DNA, in: Shuster, G. B. Ed.; Topics in Current Chemistry, vol. 236−237., Springer, Berlin, **2004**.
(16) D'Souza, F.; Deviprasad, G. R. *J. Org. Chem.* **2001**, *66*, 4601.
(17) Kurita, Y.; Takayama, C., Tanaka S. *J. Comput. Chem.* **1994**, *15*, 1013.
(18) Mulliken, R. S. *J. Am. Chem. Soc.* **1952**, *74*, 811.
(19) Sinnokrot, M. O.; Sherrill, C. D. *J. Phys. Chem. A* **2006**, *110*, 10656.
(20) Zhao, Y.; Truhlar, D. G. *Phys. Chem. Chem. Phys.* **2005**, *7*, 2701.

(21) Zhao, Y.; Truhlar, D. G. *J. Phys. Chem. A* **2005**, *108*, 6908.
(22) Zhao, Y.; Truhlar, D. G. *J. Phys. Chem. A* **2005**, *109*, 5656.
(23) Zhao, Y.; Truhlar, D. G. *J. Phys. Chem. A* **2005**, *19*, 4209.
(24) Kuboyama, A.; Nagakura, S. *J. Am. Chem. Soc.* **1955**, *77*, 2644.
(25) Bader, R. F. W. *Chem. Rev*. **1991**, *91*, 893.
(26) Bader, R. F. W. *Atoms in Molecules, a Quantum Theory*; Oxford University Press: New York, 1990.
(27) Fradera, X.; Austen, M. A.; Bader, R. F. W. *J. Chem. Phys. A* **1999**, *103*, 304.
(28) Mandado, M; González Moa, M. J.; Mosquera, R. A. *J. Comput. Chem.* **2007**, *28*, 127.
(29) Frisch, M. J.; Trucks, G. W.; Schlegel, H. B.; Scuseria, G. E.; Robb, M. A.; Cheeseman, J. R.; Montgomery, Jr., J. A.; Vreven, T.; Kudin, K. N.; Burant, J. C.; Millam, J. M.; Iyengar, S. S.; Tomasi, J.; Barone, V.; Mennucci, B.; Cossi, M.; Scalmani, G.; Rega, N.; Petersson, G. A.; Nakatsuji, H.; Hada, M.; Ehara, M.; Toyota, K.; Fukuda, R.; Hasegawa, J.; Ishida, M.; Nakajima, T.; Honda, Y.; Kitao, O.; Nakai, H.; Klene, M.; Li, X.; Knox, J. E.; Hratchian, H. P.; Cross, J. B.; Bakken, V.; Adamo, C.; Jaramillo, J.; Gomperts, R.; Stratmann, R. E.; Yazyev, O.; Austin, A. J.; Cammi, R.; Pomelli, C.; Ochterski, J. W.; Ayala, P. Y.; Morokuma, K.; Voth, G. A.; Salvador, P.; Dannenberg, J. J.; Zakrzewski, V. G.; Dapprich, S.; Daniels, A. D.; Strain, M. C.; Farkas, O.; Malick, D. K.; Rabuck, A. D.; Raghavachari, K.; Foresman, J. B.; Ortiz, J. V.; Cui, Q.; Baboul, A. G.; Clifford, S.; Cioslowski, J.; Stefanov, B. B.; Liu, G.; Liashenko, A.; Piskorz, P.; Komaromi, I.; Martin, R. L.; Fox, D. J.; Keith, T.; Al-Laham, M. A.; Peng, C. Y.; Nanayakkara, A.; Challacombe, M.; Gill, P. M. W.; Johnson, B.; Chen, W.; Wong, M. W.; Gonzalez, C.; and Pople, J. A. *Gaussian 03*, Revision C.02; Gaussian, Inc.: Wallingford, CT, 2004.
(30) Sakurai, T. *Acta. Cryst.* **1965**, *19*, 320.
(31) Williams, D. E.; Xiao, Y. *Acta. Crystallogr. Sect. A* **1998**, *49*, 1.
(32) Bader, R. F. W. *AIMPAC: A Suite of Programs for the Theory of Atoms in Molecules*; Mc Master University: Hamilton, Canada, 1994.
(33) Biegler-König, F. W.; Schönbohm, J.; Bayles, D. *J. Comp. Chem.* **2001**, *22*, 545.
(34) Hobza, P.; Sponer, J.; Reschel, T. *J. Comput. Chem.* **1995**, *16*, 1315.
(35) Cerni, J.; Hobza, P. *Phys. Chem. Chem. Phys.* **2005**, *7*, 1624.
(36) Müller-Dethlefs, K.; Hobza, P. *Chem. Rev.* **2000**, *100*, 143.
(37) Becke, A. D. *J. Chem. Phys.* **1993**, *98*, 1372.
(38) Grimme, S. *J. Chem. Phys.* **2003**, *118*, 9095.
(39) Otero, N; González Moa, M. J.; Mandado, M.; Mosquera, R. A. *Chem. Phys. Lett.* **2006**, *428*, 249.
(40) Flükiger, P. F. Ph.D. Thesis, University of Genève, Genève, France, 1992.
(41) Portmann, S.; Lüthi, H. P. *Chimia* **2000**, *54*, 766.